NASA/TM—2018-220016

Summary of the 2017 Blockage Test in the 10- by 10-Foot Supersonic Wind Tunnel

Christine Pastor-Barsi, Christopher Peters, and Manan Vyas
Glenn Research Center, Cleveland, Ohio

October 2018

NASA STI Program . . . in Profile

Since its founding, NASA has been dedicated to the advancement of aeronautics and space science. The NASA Scientific and Technical Information (STI) Program plays a key part in helping NASA maintain this important role.

The NASA STI Program operates under the auspices of the Agency Chief Information Officer. It collects, organizes, provides for archiving, and disseminates NASA's STI. The NASA STI Program provides access to the NASA Technical Report Server—Registered (NTRS Reg) and NASA Technical Report Server—Public (NTRS) thus providing one of the largest collections of aeronautical and space science STI in the world. Results are published in both non-NASA channels and by NASA in the NASA STI Report Series, which includes the following report types:

- TECHNICAL PUBLICATION. Reports of completed research or a major significant phase of research that present the results of NASA programs and include extensive data or theoretical analysis. Includes compilations of significant scientific and technical data and information deemed to be of continuing reference value. NASA counter-part of peer-reviewed formal professional papers, but has less stringent limitations on manuscript length and extent of graphic presentations.

- TECHNICAL MEMORANDUM. Scientific and technical findings that are preliminary or of specialized interest, e.g., "quick-release" reports, working papers, and bibliographies that contain minimal annotation. Does not contain extensive analysis.

- CONTRACTOR REPORT. Scientific and technical findings by NASA-sponsored contractors and grantees.

- CONFERENCE PUBLICATION. Collected papers from scientific and technical conferences, symposia, seminars, or other meetings sponsored or co-sponsored by NASA.

- SPECIAL PUBLICATION. Scientific, technical, or historical information from NASA programs, projects, and missions, often concerned with subjects having substantial public interest.

- TECHNICAL TRANSLATION. English-language translations of foreign scientific and technical material pertinent to NASA's mission.

For more information about the NASA STI program, see the following:

- Access the NASA STI program home page at http://www.sti.nasa.gov

- E-mail your question to help@sti.nasa.gov

- Fax your question to the NASA STI Information Desk at 757-864-6500

- Telephone the NASA STI Information Desk at 757-864-9658

- Write to:
  NASA STI Program
  Mail Stop 148
  NASA Langley Research Center
  Hampton, VA 23681-2199

NASA/TM—2018-220016

Summary of the 2017 Blockage Test in the 10- by 10-Foot Supersonic Wind Tunnel

Christine Pastor-Barsi, Christopher Peters, and Manan Vyas
Glenn Research Center, Cleveland, Ohio

National Aeronautics and
Space Administration

Glenn Research Center
Cleveland, Ohio 44135

October 2018

Acknowledgments

The authors would like to acknowledge and thank the test engineering and technician staff at the 10x10 SWT for their hard work and support in successfully executing the blockage test.

This work was sponsored by the Advanced Air Vehicle Program
at the NASA Glenn Research Center

Level of Review: This material has been technically reviewed by technical management.

Available from

NASA STI Program
Mail Stop 148
NASA Langley Research Center
Hampton, VA 23681-2199

National Technical Information Service
5285 Port Royal Road
Springfield, VA 22161
703-605-6000

This report is available in electronic form at http://www.sti.nasa.gov/ and http://ntrs.nasa.gov/

Summary of the 2017 Blockage Test in the 10- by 10-Foot Supersonic Wind Tunnel

Christine Pastor-Barsi, Christopher Peters, and Manan Vyas
National Aeronautics and Space Administration
Glenn Research Center
Cleveland, Ohio 44135

A limited blockage study was performed in December 2017 to explore exceeding the current published blockage curve for the NASA Glenn 10- by 10-Foot (10x10) Supersonic Wind Tunnel (SWT) at two discrete operating conditions. For the two points tested, the tunnel was found to start outside of the published starting limitations curve, above a certain threshold of Mach and stagnation pressure. Blockage theory was reviewed to further understand these results. In order to gain a firm understanding of the aerodynamic effects a more-detailed follow up blockage study is recommended.

Nomenclature

Symbols

A	area
A^*	area at the sonic condition
H	height
M	Mach number
p	pressure
W	width
δ^*	boundary-layer displacement thickness
γ	ratio of specific heats, 1.4

Subscripts

$aero$	aerodynamic cross-sectional area
$block$	cross-sectional area of the blockage caused by the model and supports
f	floor
geo	geometric cross-sectional area
$isen$	isentropic
$norm$	normal
t	throat
w	wall
0	total
1	upstream of shockwave
2	downstream of shockwave
∞	freestream condition

I. Introduction

A blockage test was performed in December 2017 to explore the possibility of testing hardware which exceeds the current published starting limitations of the 10x10 SWT, shown in Figure 1 and designated as 10x10 SWT User Manual, 2004. This experiment was not a comprehensive study as it was only two data points in excess of the current blockage curve.

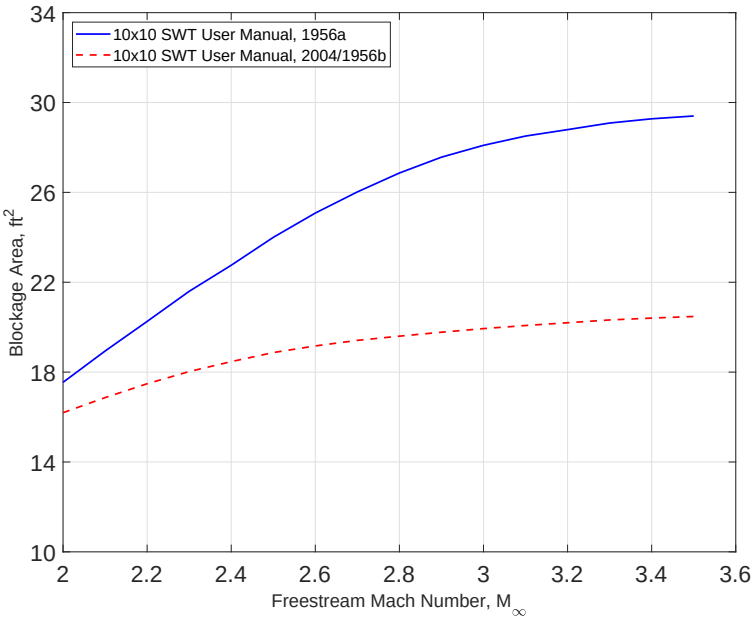

Fig. 1 Starting Limitations

In an attempt to gain some insight as to the reasoning behind the existing curve, found in reference [1], an investigation was undertaken to understand the origins of the calculated allowable test section blockage. It was found that there is sparse information to draw from in the published 10x10 SWT literature. However, there have been seven different user manuals since the facility was built in the early 1950s which provide a clue as to the time frame to focus on for investigation. It was found that all of the blockage curves are the same except for a 1956 paper copy of the "Manual for Users of the Unitary Plan Wind Tunnel Facilities of the National Advisory Committee For Aeronautics" [2]. This early version of the calculated allowable test section blockage curve is shown in Figure 1 and designated as 10x10 SWT User Manual, 1956a, which appears to match the Kantrowitz limit from Mach 2.0 through 3.2, with a discrepancy occurring above Mach 3.2. A de-rating was then performed on the curve in 1956 yielding the curve in Figure 1 designated as 10x10 SWT User Manual, 1956b, which was found in the online historical archives. There are no records detailing the rationale for de-rating the curve, however the theory behind it was investigated as part of this effort and is discussed in a subsequent section. Understanding the nature of this de-rating may help explain the results of the 2017 blockage test in which the tunnel started with a model blockage well above the original curve. It is important to note that the starting limitation curve(s) to date are understood to be calculated only and there is no record that they have ever been experimentally verified.

In the context of this paper, tunnel "start" occurs once supersonic flow is established in the diverging portion of the flexible-wall nozzle and the entirety of the test section, as indicated by the static pressure distribution in the facility. The facility is said to be "unstarted" when subsonic flow persists in any area of the flexible-wall nozzle or the test section. Previously acquired data from a 1999 calibration test (unpublished) and a 2014 Mach 4 attempt [3] provided guidelines for visual indicators and data trends of the started and unstarted condition.

The objective of this paper is to document the blockage experiment that was performed. A brief examination of blockage theory and empirical experiments performed prior to 2017 will be presented. The wind tunnel, instrumentation, model, and procedure used to conduct the blockage experiment will then be discussed. Results of the experiment will be explored within the context of the presented theory and a summary is provided. The appendices include the static pressure tap coordinates within the facility and the flexible-wall nozzle contour coordinates.

II. Theory

Figure 2 depicts various curves (theoretical and empirical) that were considered to further inform the authors about wind tunnel blockage. Typically, the first-order approach to calculating permissible blockage is the one-dimensional, inviscid, conservation of mass based theory of Kantrowitz and Donaldson [4]. This result, often referred to as the "Kantrowitz Limit," was originally derived for starting supersonic diffusers, but also applies to starting supersonic wind tunnels with partially blocked test sections since the model blockage, in the ideal sense, constricts the flow like the throat of a supersonic diffuser. Above the Kantrowitz limit, the Sun empirical correlation [5] offers a limit based on several different experiments. Taking into consideration that blunter objects exhibit greater starting difficulty [6–8], operational limits for the 1x1 SWT [9] are shown for different types of test articles based on spline fits through experimental data points. For reference, both of the 1956 curves and the current 2004 10x10 SWT blockage curve are shown.

In looking at the Kantrowitz limit further, Equation 1 defines the limit in terms of the minimum allowable area

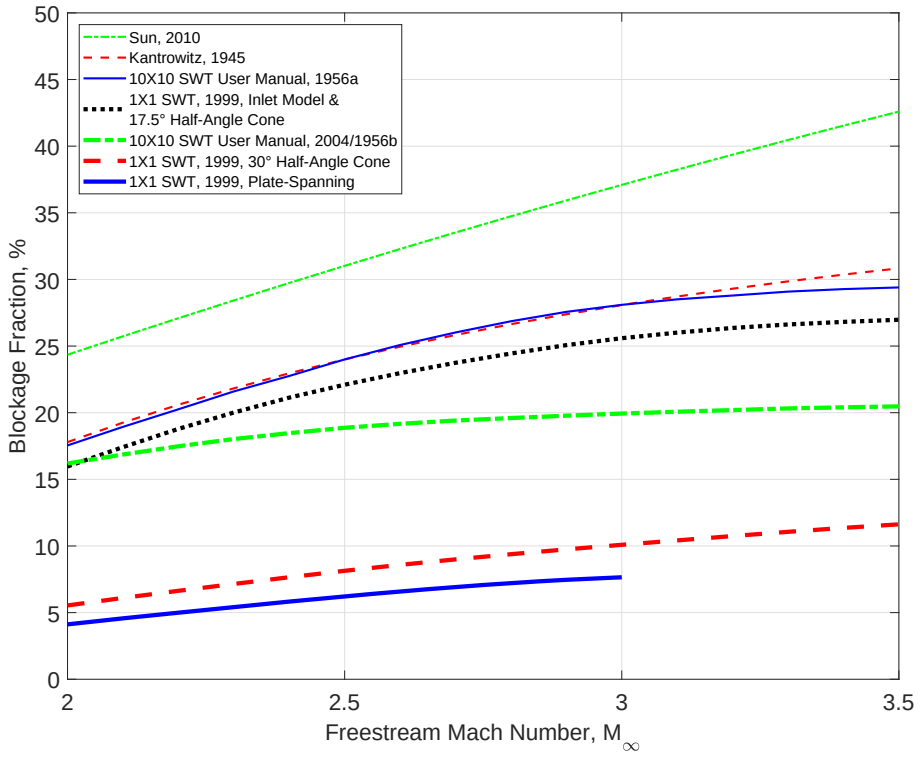

Fig. 2 Permissible Blockage Fraction for Supersonic Flow Starting: Theory, Empirical Correlations and Tunnel Recommendations

ratio, A_t/A_{geo}, necessary for starting [10].

$$\frac{A_t}{A_{geo}} = \left[\left(\frac{A^*}{A}\right)_{isen}\left(\frac{p_{01}}{p_{02}}\right)_{norm}\right]_{M=M_\infty} = \left[\frac{\gamma-1}{\gamma+1}+\frac{2}{(\gamma+1)M_\infty^2}\right]^{\frac{1}{2}}\left[\frac{2\gamma}{\gamma+1}-\frac{\gamma-1}{(\gamma+1)M_\infty^2}\right]^{\frac{1}{\gamma-1}} \tag{1}$$

The limit can be thought of as a modulation of the isentropic area ratio, (A^*/A), denoted by the subscript *isen*, by the ratio of total pressures across a normal shockwave, (p_{01}/p_{02}), denoted by subscript *norm*, with both ratios being evaluated at M_∞. According to the theory, if the flow fraction equals or exceeds this limit, the upstream normal shockwave that accompanies startup will pass the obstructing blockage (i.e., be "swallowed") and establish supersonic flow throughout the test section.

Alternatively, the Kantrowitz limit can be cast in terms of the maximum allowable blockage fraction, A_{block}/A_{geo}. This form is defined by Equation 2 and plotted in Figure 2.

$$\frac{A_{block}}{A_{geo}} \equiv \frac{A_{geo}-A_t}{A_{geo}} = 1-\frac{A_t}{A_{geo}} \tag{2}$$

The allowable blockage fraction as calculated by Kantrowitz increases with Mach number, ranging from 18% at Mach 2 up to an asymptotic value of approximately 30.0%. References [6, 11] state that the Kantrowitz limit becomes overly conservative at high Mach numbers because the startup shockwave takes on a progressively different form than a normal shockwave (see Figure 3 for the conical case) with a smaller total pressure ratio and ultimately a larger acceptable blockage fraction.

Starting exhibits hysteresis [4, 11, 12]. Holding all other tunnel parameters constant, the Mach number at which the tunnel starts from subsonic conditions is generally higher than the Mach number at which the tunnel unstarts [7]. This hysteresis phenomenon can be favorably exploited to enable testing of larger models. For example, if the model's blockage fraction at its design Mach number exceeds the limit, the tunnel can be temporarily operated at a higher Mach number until it starts and then reduced to the model's design Mach number during actual testing.

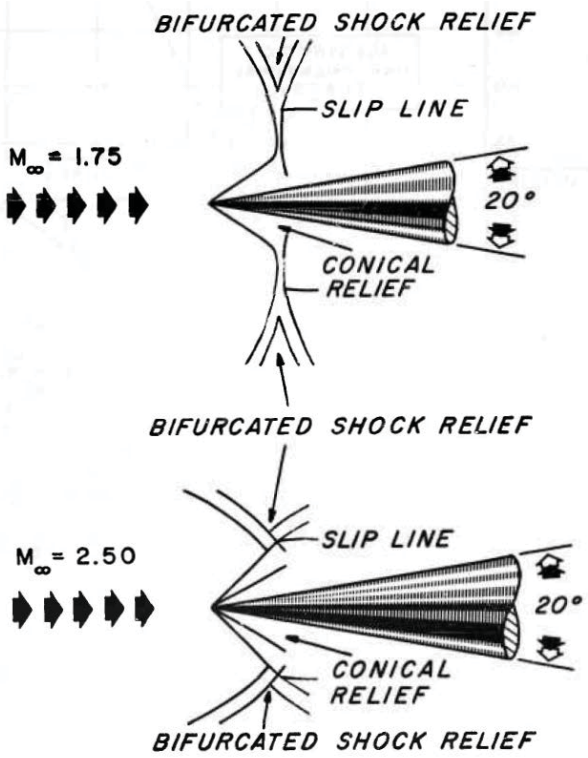

Fig. 3 Evolution of Conical Startup Shockwave with Mach number [6]

Lastly, the aerodynamic cross-sectional area, A_{aero}, defined by Equation 3, takes into account the area available for passing the flow by subtracting the area occupied by the boundary-layer displacement thickness, A_{δ^*}, from the geometric area of the test section, A_{geo}.

$$A_{aero} \equiv A_{geo} - A_{\delta^*} = W_{geo}H_{geo} - (2\delta_f^* W_{geo} + 2\delta_w^* H_{geo} - 4\delta_f^*\delta_w^*) \tag{3}$$

Equation 3 approximates A_{aero} for a rectangular test section, with W_{geo} and H_{geo} being the width (between the walls) and height (floor to ceiling), respectively, and δ_f^* and δ_w^* being the displacement thickness of the floor/ceiling and walls, respectively. Numerous references [6–8, 13–15] utilize A_{aero} instead of A_{geo} for normalizing blockage area to yield more generalizable results that are less dependent on the particular wind tunnel.

III. Infrastructure, Model, Instrumentation, and Procedure

A. 10x10 SWT Facility Description and Instrumentation

The 10x10 SWT [1] is a continuous flow, variable density wind tunnel, the layout of which is shown in Figure 4. The cross section of the test section at its inlet is 10-feet wide by 10-feet high. The test section is 40-feet long and its walls diverge $0\,^\circ 22''$ to a width of 10.51-feet at the downstream end. The floor and ceiling of the test section are parallel. There are two areas where models are positioned, the upstream and downstream stations in the test section, each of which has their own optical access for video image capture, schlieren, or laser imaging.

The nominal Mach number range within the test section is 2.0 to 3.5 and can be set to calibrated 0.1-Mach number increments. The air flow is moved through the tunnel circuit by two drive systems, each consisting of a large axial flow compressor powered by electric motors. The main drive alone is used for Mach number conditions from 2.0 to 2.5. The main drive is an eight-stage, axial-flow compressor powered by four 41,250 hp electric motors. For Mach numbers above 2.5, both the main and secondary drive systems are used. The secondary drive is a ten-stage, axial-flow compressor driven by three 41,250 hp electric motors.

The test section Mach number is controlled by the position of the flexible-wall nozzle (flexwall). The flexwall consists of two 10-foot high, 76-foot long and 1.375-inch thick stainless steel plates that are positioned by 27 stations of hydraulically operated screw-jacks. The positioning system incorporates cams on a common shaft; the cams have flats that correspond to the calibrated 0.1-Mach number increments. Measured flexwall coordinates can be found in Appendix A.

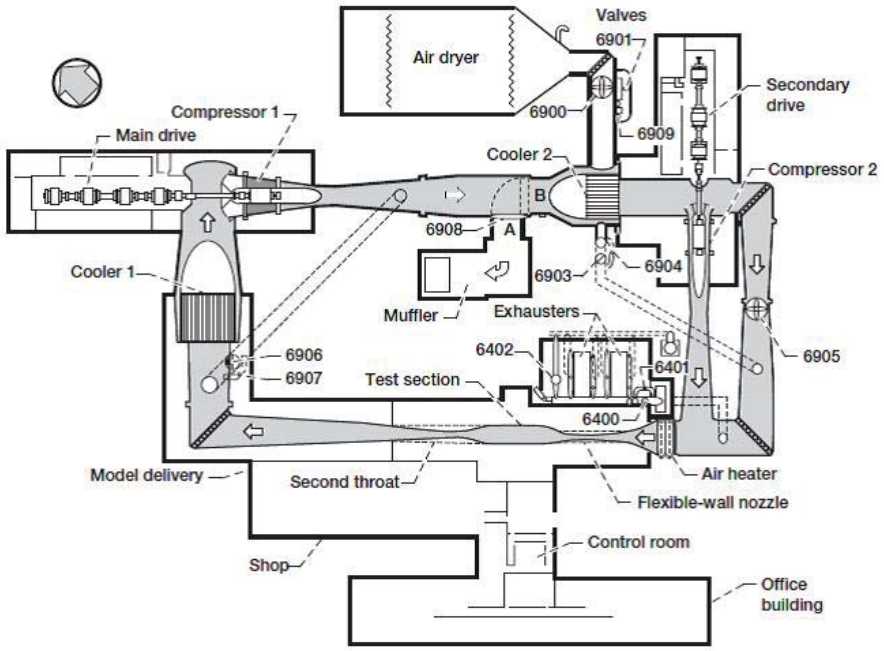

Fig. 4 10x10 Layout

The facility can be operated in either an aerodynamic cycle (closed loop) or propulsion cycle (open loop) mode. In the aerodynamic cycle, the tunnel operates in a continuous flow mode and the tunnel pressure level can be varied to provide a unit Reynolds number range of approximately 0.5 million to 3.5 million per foot. The test section total pressure varies from about 300 psfa to over 5000 psfa (about 2.5 atmospheres) with the secondary drive operating. The pressure level within the tunnel is controlled by an altitude exhaust system. In propulsion cycle, the tunnel operates at atmospheric pressure and in a continuous flow, single pass mode where the air is brought in through the air dryer, seen at the top of Figure 4, sent around the circuit and exhausted out the muffler. Propulsion cycle is used for models that introduce contaminants into the airstream, such as the products of combustion from an engine test, or when the facility's instream air heater is used. The operating mode is controlled by the positions of two valves, a 15-foot valve (inlet) and a 24-foot valve (outlet), shown as valves 6900 and 6908. The User Manual for the NASA Glenn 10- by 10-Foot Supersonic Wind Tunnel [1] details both modes of operation as well as details on the full operational envelope of the facility.

All data recorded for this test used existing facility instrumentation. The facility has four bellmouth rakes each with four total pressure probes and three thermocouples. There are also corresponding wall static pressure taps located in the same plane as the bellmouth rakes. The existing facility instrumentation includes static pressure taps that run from the flexible-wall nozzle, through the test section, and into the second throat. Figure 5(a) shows the ceiling static taps running streamwise in the flexible-wall nozzle area and the test section, while Figure 5(b) shows the facility ceiling static taps at the end of the test section and in the second throat area. Exact locations of the static taps are listed in Appendix B.

During this experiment, the tunnel was operated in aerodynamic cycle only. Steady-state data were acquired using the Escort Alpha and electronically scanned pressure (ESP) systems, standard for the 10x10 SWT. For the data presented in this report, steady-state values were averaged over 30 seconds during post-processing. No dynamic data were acquired during this test.

The bellmouth pressure measurements were made on 30 psid ESP modules, and the ceiling static pressure, flexible-wall nozzle static pressure, and the second throat static pressure measurements were all made on 15 psid ESP modules. The accuracy of the pressure measurements made with the ESP system is ±0.05% of full-scale of the module, therefore $\pm 0.03 psia$ for the 15 psid modules, and $\pm 0.045 psia$ for the 30 psid modules.

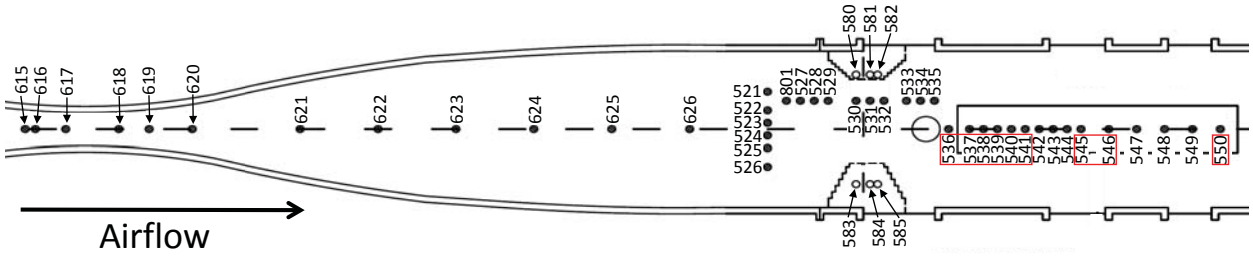

(a) Flexible-wall nozzle and Test Section Pressure Taps (Airflow is left to right). Taps identified in red squares were not in use during the experiment. Taps 580-585 are on the test section floor, all other taps are on the ceiling.

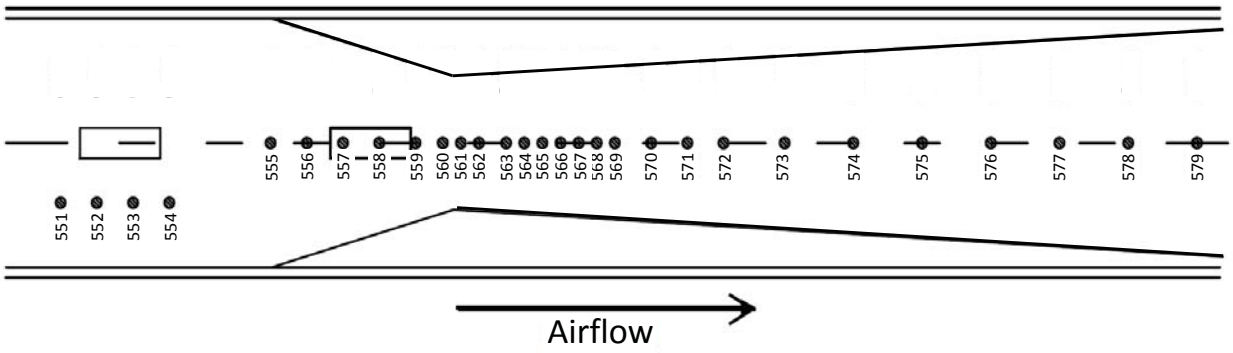

(b) Second Throat Pressure Taps (Airflow is left to right)

Fig. 5 10x10 SWT Facility Instrumentation

B. Model

There were two configurations of the blockage model which incorporated sharp leading edges and flowthrough, two features typically found on models testing in supersonic wind tunnels. For reduced complexity and ease of installation of such a large model it was mounted directly to the ceiling of the tunnel, instead of on a more typical strut. The blockage for these two configurations, with and without flowthrough, is summarized in Table 1. There was no instrumentation on the test articles. From here on out, we will only be using the blockage adjusted for flowthrough numbers (hereafter referred to as "adjusted blockage") shown in Table 1. Standard operating procedure for the facility brings the tunnel on-line with the main drive at Mach 2.0 to 2.5. Over this Mach range, the maximum permissible blockage is 16.4 ft^2 to 18.2 ft^2 in the current published curve shown in Figure 1. During standard operations the test section is started at these conditions. For this effort, this was not the case since the model frontal areas were so much larger. The facility Mach number and pressure were then increased based on a pre-determined test procedure.

Table 1 Blockage Model Values

Configuration	Geometric Blockage (ft^2)	Blockage Adjusted for flowthrough (ft^2)
1	32.4	31.0
2	36.8	35.4

C. Test Procedure

Prior to performing the experiment, several of the tunnel starting techniques that were found in the literature [16] were considered to increase the chance of success of the experiment. For example, moving the model forward was not an option due to the length of the model. However, increasing the compressor pressure ratio and opening up the second throat area were incorporated as part of the test procedure. Figure 6 shows a flow chart illustrating the test approach.

Using this pre-planned test approach/procedure, two runs of the facility were conducted. Run 1 utilized model

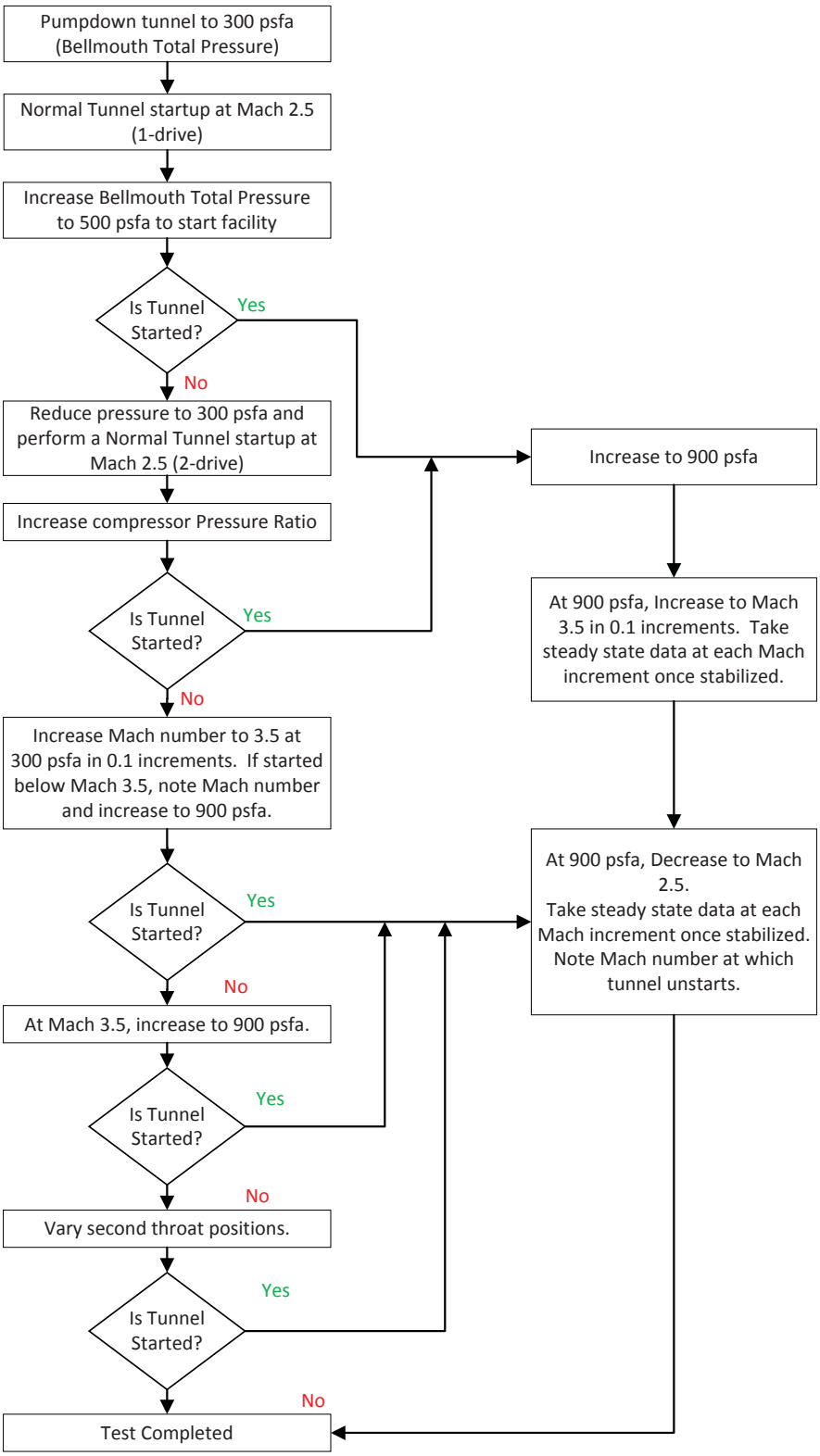

Fig. 6 Flow Chart detailing the test approach/procedures

configuration 1 with an adjusted blockage area of 31.0 ft^2 and Run 2 utilized model configuration 2 with the larger adjusted blockage area of 35.4 ft^2.

IV. Results

With configuration 1 installed in the test section and following the test procedures chart shown in Figure 6, a normal tunnel startup was performed at Mach 2.5 with a bellmouth pressure of 300 psfa and the facility did not start. The pressure level in the facility was then increased to 500 psfa at the bellmouth and the facility remained unstarted. The facility was then brought off-line to verify the integrity of the blockage model.

The facility was brought back on-line via a normal tunnel startup at Mach 2.5 for a bellmouth pressure of 300 psfa and as expected the facility remained unstarted. The compressor pressure ratios for compressors 1 and 2 were then increased and the facility remained unstarted. The tunnel Mach number was then incremented by 0.1 up to Mach 3.2 at which point the tunnel started. Visual verification of tunnel start was done using a limited schlieren view of the model. Figure 7 shows the normalized static pressure distributions in the facility from the flexible-wall nozzle, through the test section and into the second throat.

Facility bellmouth total pressure was then increased, with a target of 900 psfa, in an effort to explore the operating envelope, but at 350 psfa the facility unstarted. It is believed that the unstart resulted from the operation of compressor 1 too near its pressure ratio limit of 3.1. As tunnel total pressure started to increase, valve 6906 went into uncontrolled oscillation as it tried to keep the compressor pressure ratio below its maximum limit. After safely bringing the facility off-line, it was decided that testing would continue at nominal operational compressor pressure ratios on both compressors.

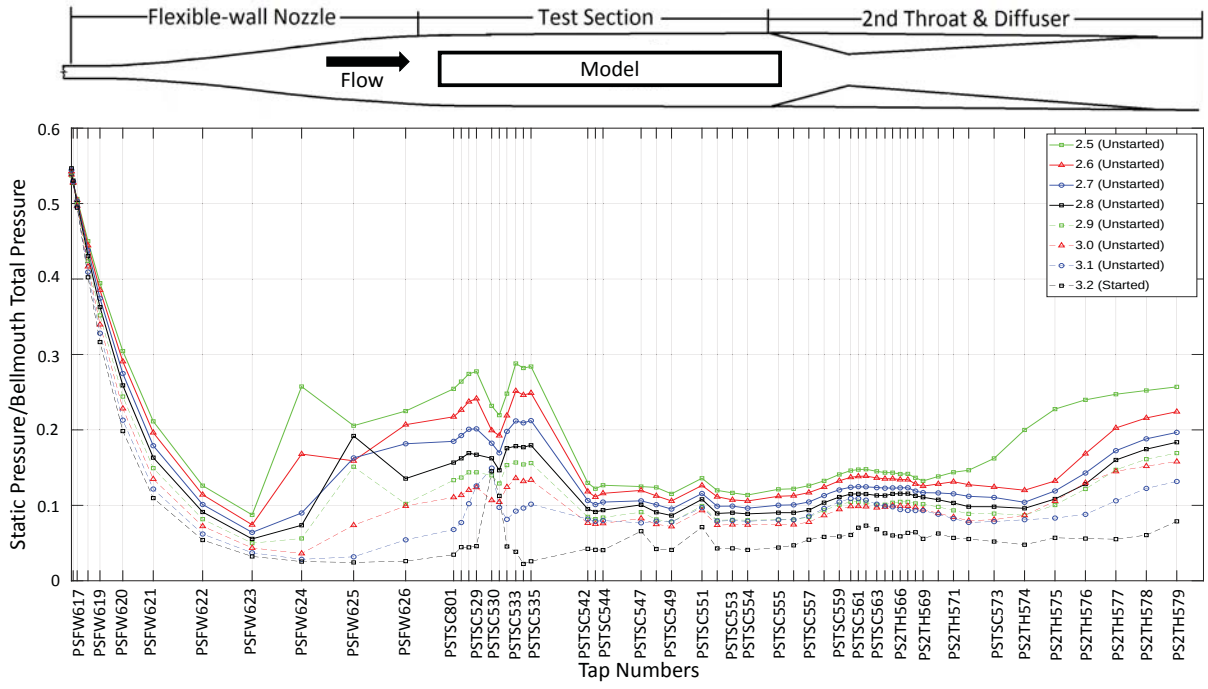

Fig. 7 Configuration 1, Bellmouth Pressure of 300 psfa, Tunnel Unstarted, Mach sweep from 2.5 to 3.2

Prior to the beginning of testing, the second throat was anticipated to be the final location for the establishment of supersonic flow and therefore the key indicator for the fully started condition. However, it was found during operations that the beginning of the test section/end of the flexible-wall nozzle was actually the last place along the observed streamwise flow path to start. This behavior indicated that the flow was choked at the blockage model, and therefore pressures PSFW625 through PSTSC801 were the key indicators used to determine tunnel start.

The facility was then brought back on-line and taken directly to Mach 3.2 at a bellmouth total pressure of 300psfa. To better characterize the hysteresis involved in the tunnel start/unstart envelope for configuration 1, starting from Mach 3.5 the tunnel Mach number was decreased by 0.1 until tunnel unstart occurred somewhere between Mach 2.8 and 2.7.

This confirmed that once started, the usable Mach number range can be expanded beyond the initial starting constraint. Figure 8 shows the tunnel started Mach numbers decremented from Mach 3.5 to 2.8.

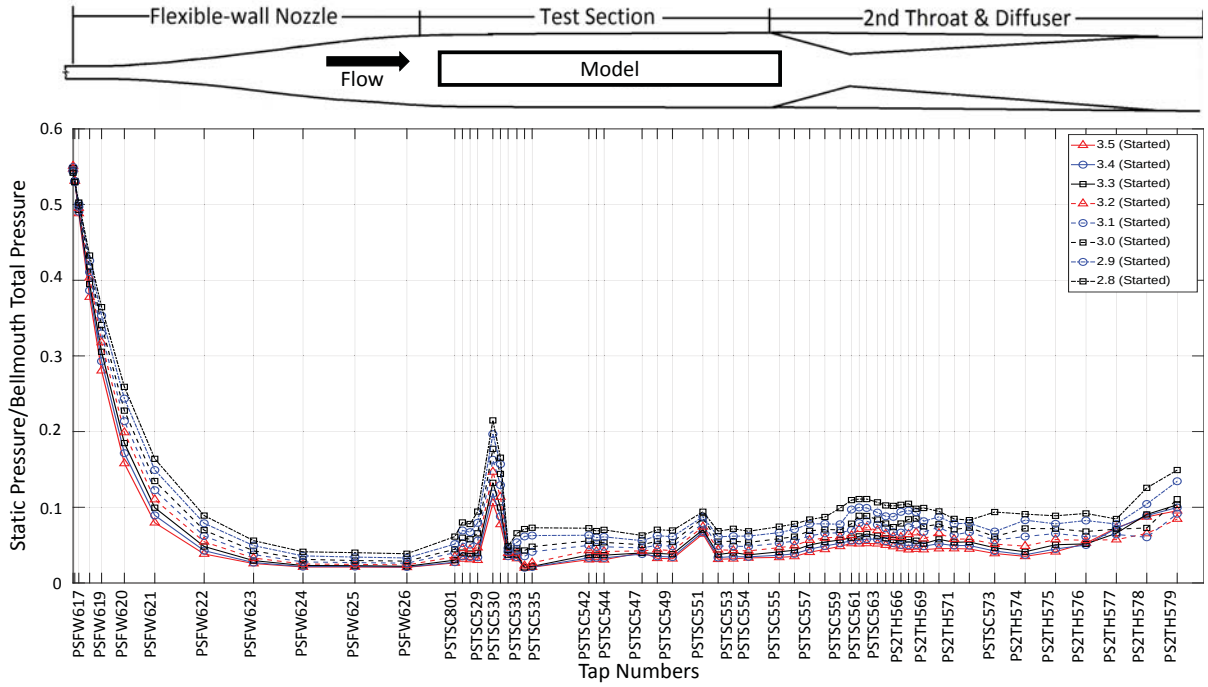

Fig. 8 Configuration 1, Bellmouth Pressure of 300 psfa, Tunnel Started, Mach sweep from 3.5 to 2.8

Run 2 utilized model configuration 2 with an adjusted blockage area of 35.4 ft^2. The run was begun with a normal tunnel startup at Mach 2.5 and a bellmouth pressure of 300 psfa and as in the previous run, the facility did not start. The tunnel Mach number was increased by 0.1 up to Mach 3.5 and the facility remained unstarted. Bellmouth total pressure was then increased to 900 psfa. On the way to 900 psfa, the tunnel started at approximately 400 psfa. Once started, the tunnel bellmouth total pressure was reduced back to 300 psfa and Mach number was decreased by 0.1 until unstart occurred somewhere between Mach 3.2 and 3.1. Figure 9 shows the started pressure distributions in the facility from the throat, through the test section and into the second throat for Mach numbers decremented from 3.5 to 3.2.

In closer examination of the data, in Figures 8-9, the flexible-wall nozzle pressure distributions were found to not agree with isentropic flow theory. Static pressure to total pressure ratios of 0.01311 at Mach 3.5 and 0.02023 at Mach 3.2 are expected, which would result in absolute static pressures of 0.027 and 0.042 psia respectively. As mentioned in a previous section, these static pressure readings were made on a 15 psid ESP module, which has an accuracy of ±0.03 psia and therefore could not discern this difference. For this particular test, this is not critical, as the objective was to look at the overall tunnel starting and blockage limits. Also, tests in the 10x10 SWT are typically not performed at a bellmouth total pressure of 300 psfa.

The facility was then taken back to Mach 3.5 and bellmouth total pressure 900 psfa to re-start. In the started condition, the bellmouth total pressure was reduced to 300 psfa to explore the impact of changing the second throat setting. The second throat area was opened larger than it's normal schedule and no impacts to the facility or flow were observed.

With the facility still in the started condition, bellmouth total pressure was increased to 900 psfa. In the started condition, at a bellmouth total pressure of 900 psfa, the tunnel Mach number was decremented by 0.1 until unstart occurred somewhere between Mach 3.0 and 2.9. Figure 10 shows the started pressure distributions in the facility from the bellmouth, through the test section and into the second throat for discrete Mach numbers decremented from 3.5 to 3.0.

The facility was then brought back to Mach 3.5, and bellmouth total pressure increased to 1200 psfa to re-start. In the started condition, while maintaining a constant bellmouth total pressure of 1200 psfa, the tunnel Mach number was decremented by 0.1 until unstart occurred somewhere between Mach 2.9 and 2.8. Figure 11 shows the started pressure

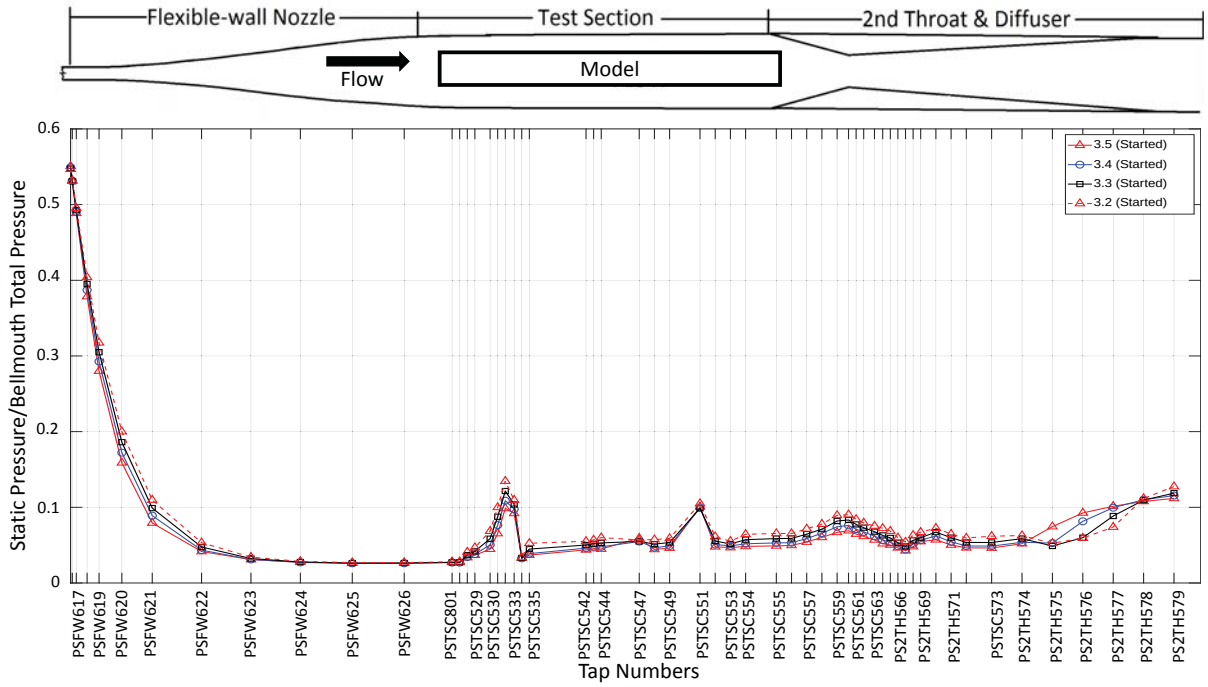

Fig. 9 Configuration 2, Bellmouth Pressure of 300 psfa, Tunnel Started, Mach sweep from 3.5 to 3.2

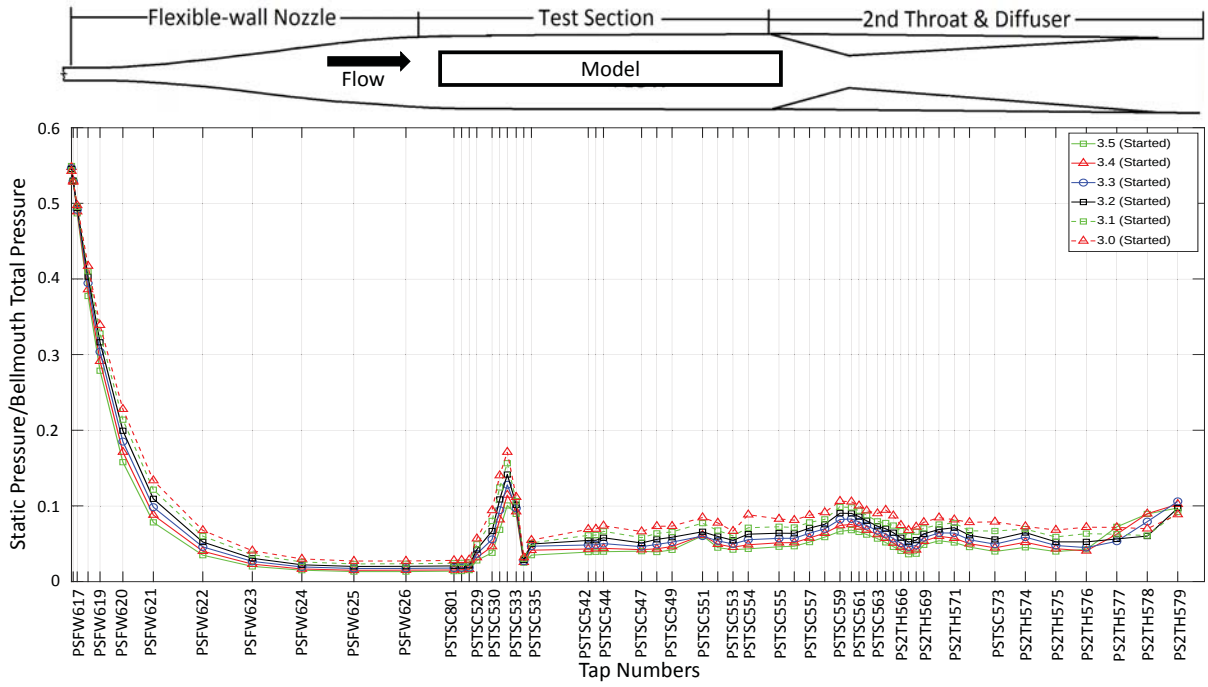

Fig. 10 Configuration 2, Bellmouth Pressure of 900 psfa, Tunnel Started, Mach sweep from 3.5 to 3.0

distributions in the facility from the bellmouth, through the test section and into the second throat for discrete Mach numbers decremented from 3.5 to 2.9. At this point, the planned test procedure was complete and the experiment was ended as operation at higher total pressures would have exceeded the blockage model hardware factors of safety.

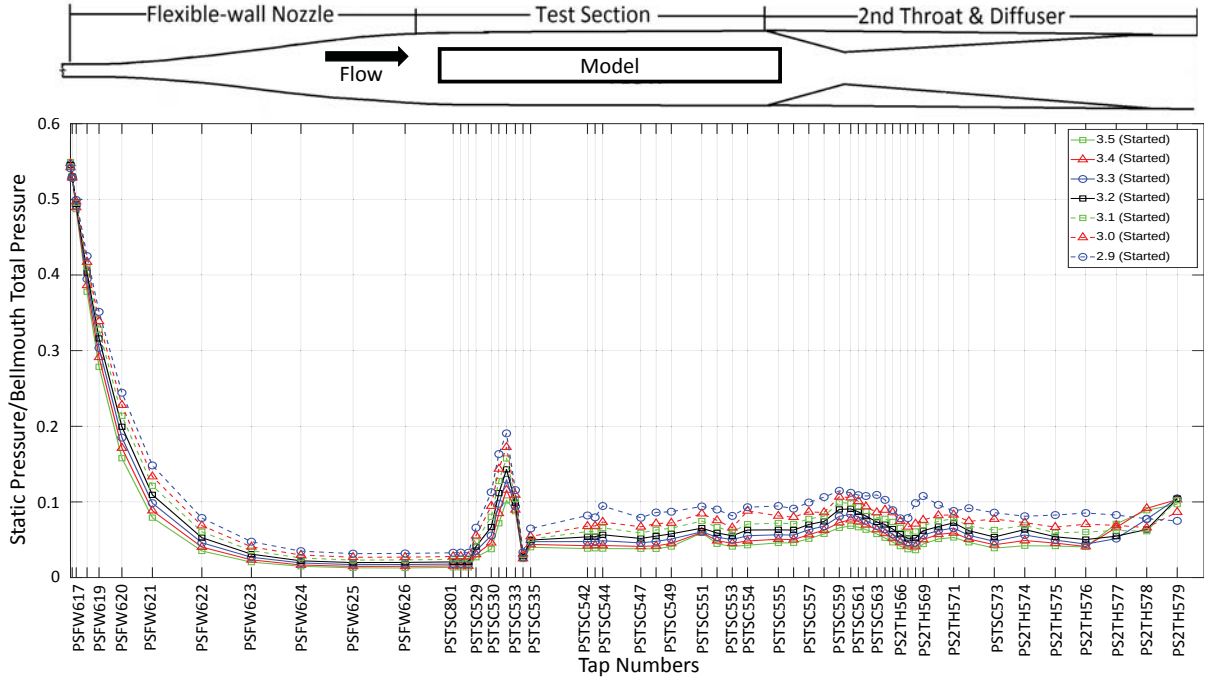

Fig. 11 Configuration 2, Bellmouth Pressure of 1200 psfa, Tunnel Started, Mach sweep from 3.5 to 2.9

Figure 12 plots the supersonic start/unstart limits with respect to pressure for the two configurations. This graph depicts the operational range of the 10x10 SWT given a particular model blockage area and total pressure. For example, with Configuration 1 (31.0 ft^2) and a total pressure of 300 psfa, the tunnel starts at Mach 3.2 and unstarts (when decrementing in Mach number, while holding pressure) between Mach 2.7 and 2.8. For Configuration 2 (35.4 ft^2), the tunnel will start at Mach 3.5 at an increased total pressure of 400 psfa, and will unstart at some lower Mach number depending on pressure. As seen in Figure 12, increased total pressure delays the Mach number at which the tunnel unstarts. The tunnel start limits that were demonstrated as part of this experiment are summarized in Table 2.

In considering blockage theory and the experiment that was just performed, Figure 13 plots several curves of calculated permissible blockage area and the experimental results associated with the largest models successfully tested in the 10x10 SWT. The upper two curves are the inviscid Kantrowitz limit and the original blockage limit found in the first 10x10 SWT user manual [2]. Their near overlap strongly suggests that the 10x10 SWT designers based early tunnel limitations on Kantrowitz theory. The lower two curves are the Kantrowitz limit based on aerodynamic cross-section and the blockage limit from the current 10x10 SWT user manual [1]. Although the Kantrowitz curve based on aerodynamic area represents the best attempt at reproducing the current limit, the noticeable discrepancy indicates that not all scaling factors were included. The data points below the current blockage limit come from the YF-12 aircraft inlet test and the combined cycle engine large scale inlet for mode transition experiment (CCE-LIMX). By design, the frontal blockage areas of these tests were below the tunnel's current limit to guarantee starting. The two data points above the Kantrowitz curve, correspond to the 2017 blockage test. In exceeding the Kantrowitz limit, these data substantiate the conservative nature of Kantrowitz theory at high Mach numbers and demonstrate that the tunnel, given sufficient total pressure, can start well above its current blockage limit for high Mach numbers.

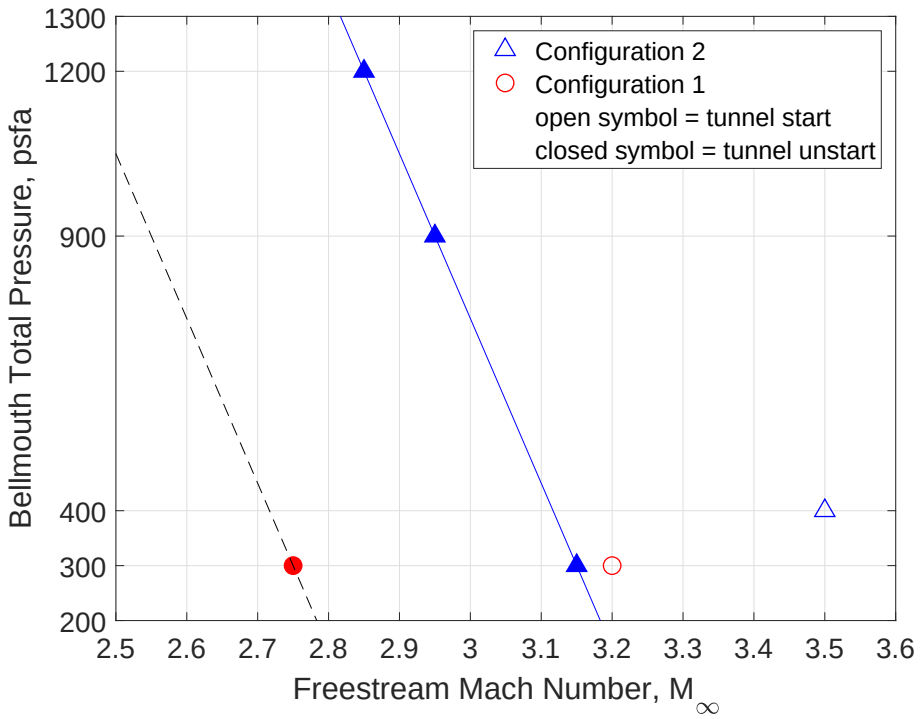

Fig. 12 Experimental Values for Starting/Unstarting with respect to Bellmouth Total Pressure

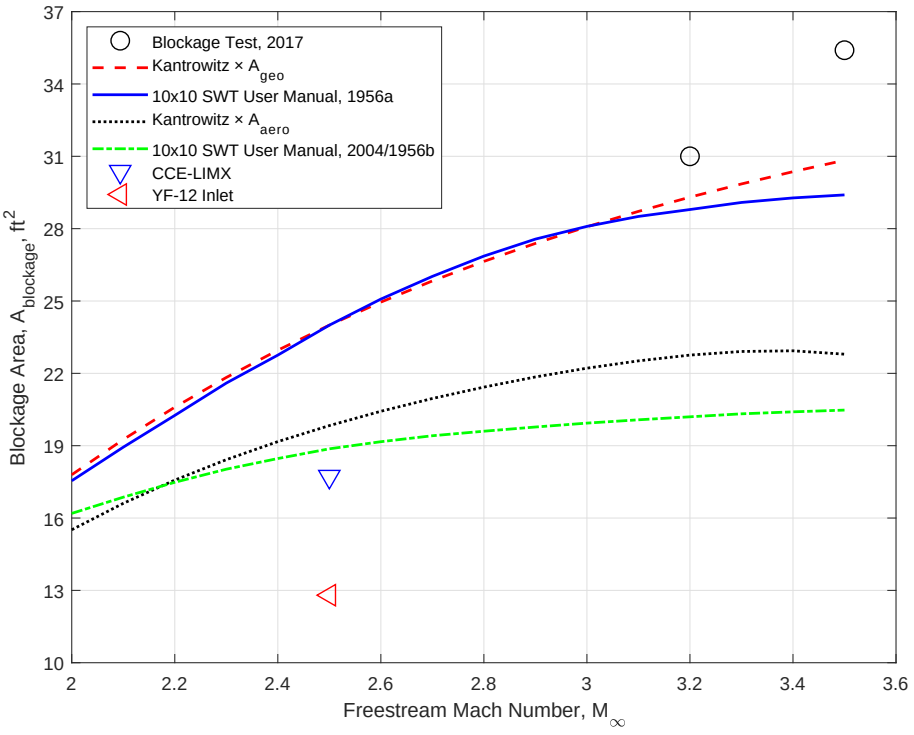

Fig. 13 10x10 SWT Permissible Blockage Area with Experimental Starting Data

Table 2 Summary of tunnel start conditions

Configuration	Adjusted Blockage Area (ft^2)	Starting Mach	Bellmouth Total Pressure (psfa)
1	31.0	3.2	300
2	35.4	3.5	approx 400

V. Summary

The blockage test, although limited in scope, demonstrated that the existing blockage curve is inadequate for fully describing the maximum size of models that can be placed in the test section without compromising the ability of the tunnel to start.

A more in-depth experimental study is recommended to explore the maximum blockage allowable for the 10x10 SWT over its entire Mach number and total pressure envelope. The information presented in this report can be used as a general guide to understand the option of exceeding the currently advertised blockage curve. Until a more in-depth study is performed, engineering staff at the 10x10 SWT facility have final say regarding any testing to be performed which would involve exceeding the currently advertised blockage curve shown in the 2004 user manual. Furthermore, this report only considers tunnel starting, no consideration is given to flow quality which may be affected by a large model (upstream propagation through the supersonic boundary-layer wave reflection impinging on the model, aerodynamic drag/wake/plume studies, etc.)

In the event another blockage test is performed in the 10x10 SWT, it is recommended that the following items be applied:

- To enable a more accurate calculation of the aerodynamic cross-section of the test section, the boundary-layer measurements for the facility as a function of Mach and Reynolds number should be updated. This will assist in future efforts to develop a revised blockage curve for the 10x10 SWT.
- To improve the ability to identify the presence of blockage effects, add static pressure instrumentation to the model external centerline and add additional facility measurements on the sidewalls and floor to identify wave impingements.

References

[1] Soeder, R. H., Roeder, J. W., Linne, A. A., and Panek, J. W., "User Manual for NASA Glenn 10- by 10-Foot Supersonic Wind Tunnel," Tech. Rep. NASA/TM-2004-212697, NASA Glenn Research Center, 2004.

[2] *The Lewis Unitary Plan Wind Tunnel*, National Advisory Committee for Aeronautics (NACA), 1956. Printed Version.

[3] Slater, J. W., and Saunders, J. D., "Increased Mach Number Capability for the NASA Glenn 10x10 Supersonic Wind Tunnel," JANNAF, 2014.

[4] Kantrowitz, A., and duPont Donaldson, C., "Preliminary Investigation of Supersonic Diffusers," Tech. Rep. NACA-ACR-L5D20, 1945.

[5] Sun, B., and Zhang, K.-Y., "Empirical Equation for Self-Starting Limit of Supersonic Inlets," *Journal of Propulsion and Power*, Vol. 26, No. 4, 2010.

[6] Draper, A. C., "Redefinition of the Limiting Concept for Supersonic Wind Tunnel Blockage," Tech. Rep. AD-155-692, June 1958.

[7] Dayman Jr., B., "Prediction of Blocking in the Supersonic Wind Tunnel during an Attempted Start," Tech. Rep. Report No. 20-109, Jet Propulsion Laboratory, June 1957.

[8] Schueler, C. J., "An Investigation of the Model Blockage for Wind Tunnels at Mach 1.5 to 19.5," Tech. Rep. AEDC-TN-59-165, 1960.

[9] Soeder, R. H., Stark, D. E., Leone, J. F., and Henry, M. W., "NASA Glenn 1- by 1-Foot Supersonic Wind Tunnel User Manual," Tech. Rep. NASA/TM-1999-208478/REV1, 1999.

[10] Flock, A. K., and Gülhan, A., "Experimental Investigation of the Starting Behavior of a three-dimensional Scramjet Intake with a Movable Cowl and Exchangeable Cowl Geometry at Different Mach Numbers," 2014. AIAA-2014-2934.

[11] Van Wie, D. M., Kwok, F. T., and Walsh, R. F., "Starting Characteristics of Supersonic Inlets," 1996.

[12] Liepmann, H. W., and Roshko, A., *Elements of Gasdynamics*, 1st ed., Dover, Mineola, New York, 2001.

[13] "Test Facilities Handbook: Policies and Procedures," Arnold Engineering Development Center (AEDC), 1959. Vol. 1.

[14] Czysz, P. A., "Correlation of Wind Tunnel Blockage Data," Tech. Rep. AD-407-689, 1963.

[15] Sverdrup Technology, Inc., "Aerodynamic Calculations for a Small Supersonic Tunnel," , October 1986. Prepared For National Aeronautics and Space Administration Lewis Research Center.

[16] Pope, A., and Goin, K. L., *High-Speed Wind Tunnel Testing*, Robert E. Krieger Publishing Company, Huntington, NY, 1978.

Appendix A. Measured Flexible-wall Nozzle Coordinates

Table A1 Measured Flexible-wall Nozzle coordinates

Flexwall Station No.	Distance upstream from TS/FW sidewall joint (inches)	Mach 2.0	Mach 2.1	Mach 2.2	Mach 2.3	Mach 2.4	Mach 2.5	Mach 2.6	Mach 2.7	Mach 2.8	Mach 2.9	Mach 3.0	Mach 3.1	Mach 3.2	Mach 3.3	Mach 3.4	Mach 3.5
North wall																	
1	862	45.067	44.504	43.907	43.378	42.886	42.367	42.06	41.706	41.397	41.132	40.867	40.672	40.479	40.32	40.169	40.041
2	829	42.668	41.661	40.582	39.603	38.686	37.755	37.099	36.407	35.788	35.234	34.688	34.279	33.871	33.504	33.185	32.88
3	794	40.345	38.889	37.332	35.911	34.577	33.188	32.242	31.219	30.293	29.45	28.64	28.009	27.387	26.825	26.329	25.868
4	759	38.257	36.405	34.436	32.617	30.918	29.148	27.926	26.616	25.411	24.32	23.272	22.443	21.633	20.905	20.245	19.646
5	724	36.537	34.36	32.053	29.91	27.914	25.814	24.378	22.823	21.402	20.105	18.858	17.872	16.908	16.039	15.253	14.539
6	690	35.288	32.881	30.332	27.952	25.741	23.397	21.812	20.079	18.499	17.056	15.652	14.557	13.482	12.511	11.631	10.821
7	660.5	34.596	32.062	29.381	26.873	24.542	22.074	20.397	18.568	16.899	15.373	13.889	12.734	11.595	10.565	9.633	8.775
8	631	34.361	31.772	29.045	26.489	24.114	21.605	19.888	18.023	16.318	14.759	13.253	12.059	10.896	9.842	8.889	8.018
9	601.5	34.6	32.055	29.372	26.859	24.52	22.056	20.356	18.515	16.835	15.295	13.815	12.628	11.473	10.435	9.494	8.644
10	571	35.304	32.881	30.331	27.945	25.717	23.382	21.752	20.002	18.395	16.923	15.525	14.374	13.27	12.28	11.379	10.583
11	537	36.561	34.399	32.082	29.92	27.892	25.737	24.27	22.671	21.198	19.852	18.549	17.513	16.503	15.595	14.766	14.027
12	502	38.309	36.49	34.493	32.626	30.858	28.953	27.695	26.291	24.997	23.803	22.642	21.748	20.853	20.056	19.322	18.692
13	469	40.303	38.845	37.193	35.651	34.163	32.544	31.48	30.28	29.168	28.142	27.148	26.375	25.601	24.915	24.291	23.813
14	442.5	42.125	40.969	39.628	38.37	37.127	35.732	34.838	33.805	32.838	31.949	31.079	30.416	29.741	29.145	28.604	28.236
15	417	44.004	43.157	42.119	41.13	40.117	38.947	38.203	37.318	36.479	35.707	34.963	34.371	33.781	33.262	32.795	32.495
16	391.5	45.985	45.487	44.755	44.037	43.246	42.238	41.67	40.913	40.19	39.709	38.839	38.364	37.847	37.399	36.991	36.646
17	366	48.022	47.867	47.435	46.965	46.368	45.477	45.044	44.364	43.72	43.147	42.521	42.14	41.687	41.287	40.924	40.549
18	338.5	50.252	50.443	50.287	49.989	49.492	48.647	48.325	47.674	47.105	46.649	46.092	45.808	45.41	45.041	44.719	44.337

Continued on next page

Flexwall Station No.	Distance upstream from TS/FW sidewall joint (inches)	Mach 2.0	Mach 2.1	Mach 2.2	Mach 2.3	Mach 2.4	Mach 2.5	Mach 2.6	Mach 2.7	Mach 2.8	Mach 2.9	Mach 3.0	Mach 3.1	Mach 3.2	Mach 3.3	Mach 3.4	Mach 3.5
19	309	52.615	53.038	52.994	52.752	52.298	51.51	51.3	50.686	50.189	49.877	49.397	49.21	48.856	48.524	48.224	47.861
20	276	54.913	55.339	55.326	55.135	54.744	54.107	53.981	53.416	53.013	52.853	52.486	52.362	52.054	51.746	51.46	51.159
21	242	56.736	57.008	56.998	56.869	56.573	56.137	56.062	55.568	55.265	55.239	54.991	54.864	54.597	54.318	54.047	53.908
22	208	57.998	58.126	58.113	58.045	57.846	57.592	57.568	57.175	56.966	57.016	56.839	56.708	56.483	56.249	56.011	56.048
23	174	58.75	58.789	58.772	58.749	58.658	58.538	58.549	58.298	58.175	58.221	58.091	57.979	57.815	57.634	57.447	57.608
24	140	59.125	59.125	59.111	59.11	59.095	59.062	59.079	58.992	58.938	58.943	58.872	58.794	58.692	58.572	58.435	58.652
25	105	59.364	59.352	59.34	59.346	59.351	59.35	59.392	59.404	59.39	59.388	59.366	59.327	59.277	59.212	59.13	59.313
26	70	59.478	59.464	59.458	59.454	59.465	59.474	59.514	59.543	59.534	59.533	59.534	59.514	59.5	59.464	59.414	59.528
27	35	59.764	59.746	59.744	59.743	59.746	59.76	59.768	59.781	59.779	59.779	59.793	59.778	59.777	59.766	59.745	59.786
TS	0	60.005	60.005	60.005	60.005	60.005	60.005	60.005	60.005	60.005	60.005	60.005	60.005	60.005	60.005	60.005	60.005
South wall																	
1	862	45.06	44.496	43.897	43.37	42.875	42.391	42.059	41.704	41.392	41.126	40.855	40.667	40.472	40.316	40.164	40.025
2	829	42.697	41.687	40.606	39.63	38.715	37.762	37.133	36.453	35.828	35.277	34.735	34.324	33.922	33.562	33.236	32.942
3	794	40.331	38.875	37.322	35.901	34.568	33.174	32.238	31.217	30.29	29.45	28.641	28.004	27.385	26.828	26.328	25.874
4	759	38.256	36.399	34.429	32.61	30.908	29.134	27.92	26.605	25.409	24.32	23.274	22.44	21.635	20.9	20.247	19.654
5	724	36.545	34.363	32.059	29.915	27.918	25.823	24.388	22.831	21.414	20.118	18.872	17.883	16.92	16.045	15.257	14.549
6	690	35.304	32.89	30.343	27.961	25.749	23.411	21.821	20.092	18.506	17.056	15.668	14.569	13.489	12.515	11.635	10.839
7	660.5	34.606	32.063	29.385	26.877	24.544	22.083	20.4	18.572	16.902	15.376	13.9	12.731	11.594	10.561	9.629	8.787
8	631	34.348	31.765	29.038	26.484	24.109	21.605	19.882	18.021	16.314	14.754	13.252	12.053	10.89	9.831	8.878	8.018
9	601.5	34.602	32.059	29.377	26.865	24.527	22.066	20.366	18.527	16.847	15.307	13.826	12.639	11.486	10.447	9.503	8.653
10	571	35.305	32.897	30.345	27.958	25.731	23.383	21.766	20.014	18.411	16.939	15.521	14.393	13.284	12.293	11.393	10.584
11	537	36.574	34.41	32.094	29.929	27.897	25.749	24.275	22.673	21.206	19.857	18.551	17.521	16.506	15.592	14.765	14.037

Continued on next page

Flexwall Station No.	Distance upstream from TS/FW sidewall joint (inches)	Mach 2.0	Mach 2.1	Mach 2.2	Mach 2.3	Mach 2.4	Mach 2.5	Mach 2.6	Mach 2.7	Mach 2.8	Mach 2.9	Mach 3.0	Mach 3.1	Mach 3.2	Mach 3.3	Mach 3.4	Mach 3.5
12	502	38.318	36.485	34.485	32.622	30.853	28.954	27.686	26.279	24.985	23.795	22.633	21.734	20.842	20.038	19.314	18.687
13	469	40.315	38.848	37.199	35.659	34.176	32.549	31.49	30.286	29.175	28.15	27.142	26.378	25.606	24.918	24.293	23.807
14	442.5	42.127	40.97	39.626	38.369	37.127	35.738	34.844	33.803	32.842	31.95	31.07	30.415	29.738	29.141	28.599	28.231
15	417	44.006	43.18	42.145	41.16	40.149	38.95	38.235	37.35	36.519	35.747	34.956	34.413	33.822	33.302	32.835	32.504
16	391.5	45.996	45.484	44.754	44.039	43.25	42.263	41.676	40.919	40.197	39.748	38.853	38.366	37.854	37.398	36.994	36.668
17	366	48.019	47.862	47.437	46.97	46.361	45.468	45.043	44.358	43.719	43.144	42.503	42.135	41.678	41.273	40.915	40.535
18	338.5	50.246	50.437	50.286	49.984	49.487	48.635	48.32	47.67	47.096	46.643	46.075	45.798	45.392	45.029	44.703	44.315
19	309	52.632	53.051	53.006	52.759	52.306	51.53	51.306	50.689	50.193	49.88	49.412	49.216	48.86	48.524	48.225	47.873
20	276	54.91	55.33	55.315	55.122	54.735	54.092	53.97	53.404	53.005	52.845	52.476	52.353	52.044	51.733	51.449	51.149
21	242	56.732	57.033	57.017	56.89	56.595	56.137	56.085	55.59	55.291	55.261	55.005	54.895	54.622	54.34	54.066	53.91
22	208	57.994	58.138	58.126	58.057	57.861	57.587	57.587	57.193	56.987	57.036	56.843	56.731	56.503	56.266	56.029	56.054
23	174	58.738	58.781	58.762	58.739	58.647	58.525	58.543	58.29	58.167	58.213	58.081	57.97	57.803	57.626	57.433	57.601
24	140	59.086	59.092	59.076	59.075	59.058	59.023	59.045	58.953	58.899	58.908	58.841	58.74	58.653	58.537	58.402	58.619
25	105	59.28	59.272	59.259	59.261	59.267	59.268	59.309	59.321	59.308	59.303	59.287	59.244	59.191	59.126	59.045	59.234
26	70	59.5	59.487	59.478	59.475	59.483	59.496	59.533	59.56	59.553	59.553	59.554	59.533	59.515	59.48	59.432	59.55
27	35	59.758	59.75	59.747	59.744	59.747	59.756	59.77	59.782	59.779	59.779	59.788	59.777	59.775	59.765	59.743	59.782
TS	0	60.005	60.005	60.005	60.005	60.005	60.005	60.005	60.005	60.005	60.005	60.005	60.005	60.005	60.005	60.005	60.005

Appendix B. Static Tap Station Locations

X values are in the axial direction. Y values are in the vertical direction. Z values are in the horizontal direction.

Table B1 Facility Static Tap Locations as measured from the Test Section Datum (inches)

Channel Name	Description	X	Y	Z
PSFW615	Flexwall Static Pressure (615)	-668.4375	60	-2
PSFW616	Flexwall Static Pressure (616)	-665.75	60	-2
PSFW617	Flexwall Static Pressure (617)	-659.4375	60	-2
PSFW618	Flexwall Static Pressure (618)	-642.375	60	-2
PSFW619	Flexwall Static Pressure (619)	-623.5	60	-2
PSFW620	Flexwall Static Pressure (620)	-587.5	60	-2
PSFW621	Flexwall Static Pressure (621)	-539.5	60	-2
PSFW622	Flexwall Static Pressure (622)	-461.625	60	-2
PSFW623	Flexwall Static Pressure (623)	-383.625	60	-2
PSFW624	Flexwall Static Pressure (624)	-305.625	60	-2
PSFW625	Flexwall Static Pressure (625)	-223.625	60	-2
PSFW626	Flexwall Static Pressure (626)	-141.625	60	-2
PSTSC521	Test Section Ceiling Static Pressure (521)	-78	60	-36
PSTSC522	Test Section Ceiling Static Pressure (522)	-78	60	-18
PSTSC523	Test Section Ceiling Static Pressure (523)	-78	60	-6
PSTSC524	Test Section Ceiling Static Pressure (524)	-78	60	6
PSTSC525	Test Section Ceiling Static Pressure (525)	-78	60	18
PSTSC526	Test Section Ceiling Static Pressure (526)	-78	60	36
PSTSC801	Test Section Ceiling Static Pressure (801)	-66	60	-24
PSTSC527	Test Section Ceiling Static Pressure (527)	-54	60	-24
PSTSC528	Test Section Ceiling Static Pressure (528)	-42	60	-24
PSTSC529	Test Section Ceiling Static Pressure (529)	-30	60	-24
PSTSC530	Test Section Ceiling Static Pressure (530)	-6	60	-24
PSTSC531	Test Section Ceiling Static Pressure (531)	6	60	-24
PSTSC532	Test Section Ceiling Static Pressure (532)	18	60	-24
PSTSC533	Test Section Ceiling Static Pressure (533)	32	60	-24
PSTSC534	Test Section Ceiling Static Pressure (534)	44	60	-24
PSTSC535	Test Section Ceiling Static Pressure (535)	56	60	-24
PSTSC536	Test Section Ceiling Static Pressure (536)	68	60	0
PSTSC537	Test Section Ceiling Static Pressure (537)	85.5	60	0
PSTSC538	Test Section Ceiling Static Pressure (538)	97.5	60	0
PSTSC539	Test Section Ceiling Static Pressure (539)	109.5	60	0
PSTSC540	Test Section Ceiling Static Pressure (540)	121.5	60	0
PSTSC541	Test Section Ceiling Static Pressure (541)	133.5	60	0
PSTSC542	Test Section Ceiling Static Pressure (542)	145.5	60	0
PSTSC543	Test Section Ceiling Static Pressure (543)	157.5	60	0

Continued on next page

Channel Name	Description	X	Y	Z
PSTSC544	Test Section Ceiling Static Pressure (544)	169.5	60	0
PSTSC545	Test Section Ceiling Static Pressure (545)	181.5	60	0
PSTSC546	Test Section Ceiling Static Pressure (546)	205.5	60	0
PSTSC547	Test Section Ceiling Static Pressure (547)	229.5	60	0
PSTSC548	Test Section Ceiling Static Pressure (548)	253.5	60	0
PSTSC549	Test Section Ceiling Static Pressure (549)	277.5	60	0
PSTSC550	Test Section Ceiling Static Pressure (550)	301.5	60	0
PSTSC551	Test Section Ceiling Static Pressure (551)	325.5	60	-24
PSTSC552	Test Section Ceiling Static Pressure (552)	349.5	60	-24
PSTSC553	Test Section Ceiling Static Pressure (553)	373.5	60	-24
PSTSC554	Test Section Ceiling Static Pressure (554)	397.5	60	-24
PSTSC555	2nd Throat Ceiling Static Pressure (555)	446	60	-18
PSTSC556	2nd Throat Ceiling Static Pressure (556)	470	60	-18
PSTSC557	2nd Throat Ceiling Static Pressure (557)	494	60	-18
PSTSC558	2nd Throat Ceiling Static Pressure (558)	518	60	-18
PSTSC559	2nd Throat Ceiling Static Pressure (559)	542	60	-18
PSTSC560	2nd Throat Ceiling Static Pressure (560)	560	60	-18
PSTSC561	2nd Throat Ceiling Static Pressure (561)	572	60	-18
PSTSC562	2nd Throat Ceiling Static Pressure (562)	584	60	-18
PSTSC563	2nd Throat Ceiling Static Pressure (563)	601	60	-18
PSTSC564	2nd Throat Ceiling Static Pressure (564)	614	60	-18
PSTSC565	2nd Throat Ceiling Static Pressure (565)	626	60	-18
PSTSC566	2nd Throat Ceiling Static Pressure (566)	638	60	-18
PSTSC567	2nd Throat Ceiling Static Pressure (567)	650	60	-18
PSTSC568	2nd Throat Ceiling Static Pressure (568)	662	60	-18
PSTSC569	2nd Throat Ceiling Static Pressure (569)	674	60	-18
PSTSC570	2nd Throat Ceiling Static Pressure (570)	698	60	-18
PSTSC571	2nd Throat Ceiling Static Pressure (571)	722	60	-18
PSTSC572	2nd Throat Ceiling Static Pressure (572)	746	60	-18
PSTSC573	2nd Throat Ceiling Static Pressure (573)	786	60	-18
PSTSC574	2nd Throat Ceiling Static Pressure (574)	834	60	-18
PSTSC575	2nd Throat Ceiling Static Pressure (575)	882	60	-18
PSTSC576	2nd Throat Ceiling Static Pressure (576)	930	60	-18
PSTSC577	2nd Throat Ceiling Static Pressure (577)	978	60	-18
PSTSC578	2nd Throat Ceiling Static Pressure (578)	1026	60	-18
PSTSC579	2nd Throat Ceiling Static Pressure (579)	1074	60	-18